

# Proposal of 3D Micro Prototyping Using Synchrotron Radiation and Its Application to Bio-Microsystems

Yuichi Utsumi

Laboratory of Advanced Science and Technology for Industry , University of Hyogo, Kamigori, Ako, Hyogo, Japan

## Abstract

A new X-ray microfabrication system and succeeding molding process as the 3D micro prototyping process have been developed using synchrotron radiation (SR) lithography and nano-imprinting technique. We adapted the process to the achievement of 3D microfluidic platforms for bio chemical applications which will be used point-of-care diagnostics and drug compound screenings. An enzyme linked immunosorbent assay method has been applied to the analysis of the endocrine disrupter using proposed fluidic platforms. Drastic improvement of the analysis sensitivity and decreasing of the total analysis effort and required time have confirmed

## Keywords:

synchrotron radiation; microfabrication; microfluidics; Lab on chip; assay ; ELISA ;DNA

## 1 INTRODUCTION

There have been rapid developments in the application of microsystems in advanced industries such as intelligent information systems, energy and environment conservations, and medical and biochemical applications. Microsystems typically consist of different types of precise parts for various micro structures. The realization of 3D microstructures integrating multiple functions, such as electrical, optical, mechanical, and chemical sequential operations, in a restricted space will bring many advantages to the industry development. Systems of this type have been fabricated using micro-electro-mechanical system (MEMS) processes. Recently, however, fabrication techniques with a higher precision and a higher aspect ratio than those conventionally achievable have become increasingly important. This is due to the fact that natural phenomena on which these device functions are based, such as electrostatic fields, surface tension, and surface chemical reactions, tend to become more pronounced as specific surface area increases. To realize these requirement, we developed a new "3D micro prototyping process" based on X-ray microfabrication system equipped at the "NewSUBARU" SR facility [1,2]. and succeeding molding process using synchrotron radiation (SR) lithography and nano-imprinting technique. The stacking process as the device packaging of obtained micro structures is more essential where it needs various surface treatment and succeeding bonding process with different materials [3,4]. Meanwhile, the progress of life science has been increasing rapidly and the development of the platform technologies that supports it become more significant. Miniaturization and integration technology that have been successfully developed at microelectronics fields are nowadays adapting also to automated chemical analysis and synthesis, based on miniaturized total chemical system, so-called "μTAS " or "Lab on Chip" made from microfluidic components. We adapted proposed "3D micro prototyping process" to the achievement of the integrated microfluidic platform and have confirmed advantages of 3D micro-integration of chemical functions in one platform for some biochemical applications. A high sensitive and rapid enzyme linked immunosorbent assay (ELISA) method are demonstrated using micro 3D-structured

system consists of 3D microfluidic channel network and vertical chemical operation chamber with fluid control filter and mixer. Drastic improvement of the analysis sensitivity and decreasing the total analysis effort and required time have found in the applications to the environmental analysis and DNA analysis.

## 2 3D MICRO PROTOTYPING USING SYNCHROTRON RADIATION

### 2.1 3D X-ray Microfabrication System

The "lithographie, galvanofornung, abformung" (LIGA) process, which consists of deep-X-ray lithography, electroforming, and molding, is a promising candidate for 3D microfabrication[5]. The LIGA process starts from the fabrication of high-aspect-ratio polymer microstructures with heights greater than a few hundred microns using deep-X-ray lithography of a photosensitive polymer (resist) [6]. In the next step, a metal replica structure is formed by electroforming using the fabricated polymer master. The obtained metal replica structure can be used as a component in a

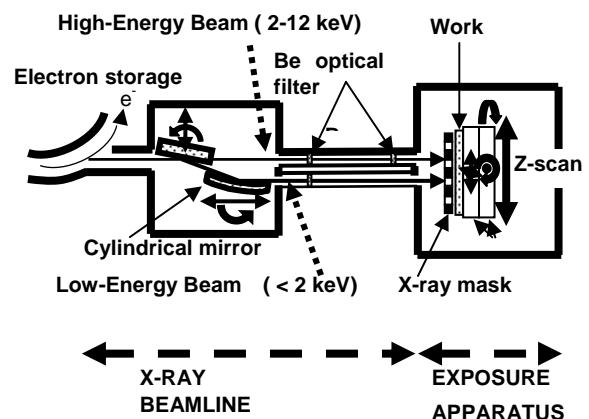


Figure 1: Schematic diagram of newly developed lithography system using SR.

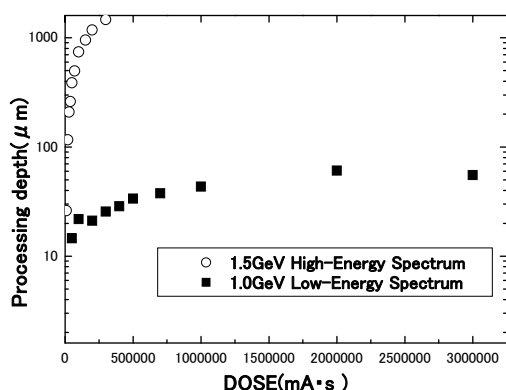


Figure 2: Exposure-dose dependence of processing depth. Circles show the data using the high-energy spectrum for 1.5 GeV operation. Squares show the data using the low-energy spectrum for 1.0 GeV operation.

microsystem or as a mold insert for final molding processes, such as hot embossing and injection molding. It is important to develop a next-generation process that can achieve both a large process area and more fine fabrication property simultaneously. No such process satisfying the demands has yet been realized. We established a new X-ray lithography system, “BL2”, with a large exposure area of up to A4 size, developed at the “NewSUBARU” synchrotron radiation facility [2]. Figure 1 shows a schematic diagram of the newly developed apparatus for lithography. It consists of a beamline with X-ray optics for energy selection and an exposure apparatus with multi motion stages. The main feature of our lithography system is that it can continuously select X-rays from 1 to 12 keV using mirrors and the filters. Each energy region can be selected in accordance with the desired size and shape of the fabricated microstructures. Figure 2 shows the relationship between the processing depth of a PMMA resist after 3 h of development and the X-ray exposure dose at operation energies of 1.0 and 1.5 GeV. A processing depth of more than 1600  $\mu\text{m}$  was obtained with exposure to the high-energy X-ray beam during 1.5 GeV operation. It is clearly shown that exposure photon energy changes dose dependence on processing depth of the work (PMMA), since the penetration depth of the X-rays into the resist varies according to their energy. By scanning the 210-mm-wide SR beam along the longitudinal axis with a 800 mm span, full A4-size exposure can be achieved. Figure 3 shows that

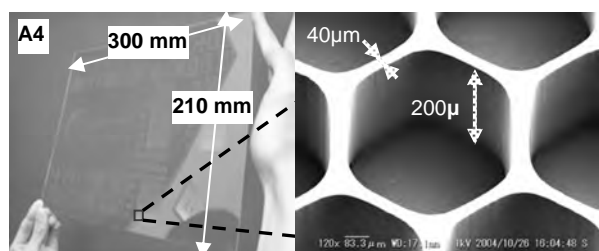


Figure 3: PMMA resist patterns fabricated using large-area deep x-ray lithography system. A4-size deep x-ray lithography, and right magnified image shows patterns with high accuracy.

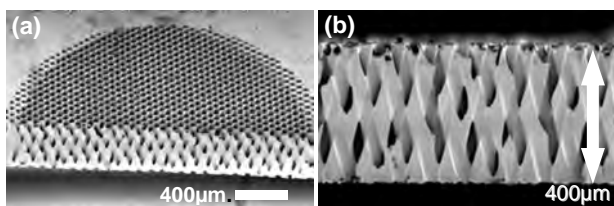


Figure 4: (a); Three-dimensional microstructures patterned on a 400 micron PMMA sheet using SR with multi step exposure. (b); magnified image of the cross-linked micro capillaries.

large-area patterning of an area of 220 mm  $\times$  300 mm (A4-size) with a highly uniform pattern thickness is successfully demonstrated using this system. The uniformity of the pattern thickness along the horizontal direction was estimated to be less than 5%. Patterning with an aspect ratio greater than 20 was confirmed. Using this large-area X-ray lithography system, high-aspect-ratio microstructures with a wide range of sizes, from submicron to millimeter, can be achieved by using different type of X-ray masks in the same exposure chamber.

In order to apply this system to the fabrication of advanced microsystems with more integrated functions for automated operations, it is necessary to develop a high-precision 3D microfabrication technique capable of sizes less than several dozen of microns. Several 3D microfabrication studies have been reported so far [7-8]. In this study, three-dimensional microstructures can be obtained by exposing the X-ray beam intermittently over work substrate (PMMA) with different incident SR angles set by multi axis stages [9] as shown in Figure 4 (a), (b). This structure shows the cross-linked micro capillaries for mixing of micro fluids with small Reynolds number, where high mixing efficiency was confirmed from the reaction speed measurement of the enzyme and substrate solution [10]. This 3D structure of cross-linked micro capillaries can be fabricated by tilting the exposure stage. The 400 $\mu\text{m}$  thick PMMA sheet and X-ray mask are mounted on an X-ray exposure stage, and the stage is tilted from the vertical axis, and PMMA sheet is exposed to X-ray. Then, the stage is reversely tilted by same angle and exposed again. The distance between crossing axes of the capillaries can be controlled by rotating the X-ray mask a few degrees. The mixing efficiency was significantly affected by the distance between center axes of each capillary. Figure 5 (a) shows the results of the computational fluid dynamics (CFD) simulation of water mixed after 0.5 ms, which suggests the great improvement of the mixing efficiency by using this 3D structured capillaries. The color bar indicates mass fraction of the colored water. Figure 5 (b) shows time shift of standard deviation of the mass fraction of the ideal separated waters in poured from both side of the two cross-linked capillaries and mixed in capillaries as the mixing progress. The capillary structural parameter is 40  $\mu\text{m}$  and 400 $\mu\text{m}$  in diameter and length. The result shows that mixing efficiency in cross-linked capillary is much increased at the structure of which distance between center axes of each capillary is half in diameter (half cross-linked structure). Moreover, the mixing will be finished within 1 ms by the use of the mixer with half cross-linked micro capillaries.

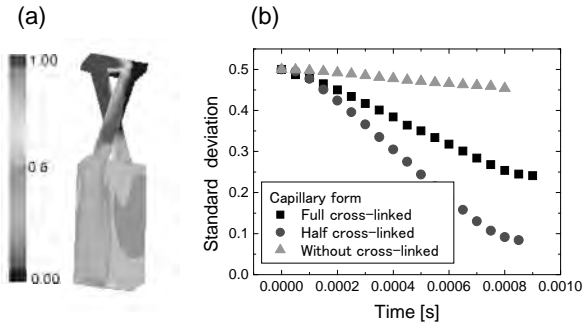


Figure 5: (a); Simulated mixing behavior. (b); time shift of standard deviation of the mass fraction of the ideal separated waters in poured from both side of the two cross-linked capillaries.

## 2.2 Microfabrication of PTFE by SR-induced Direct Etching

The X-ray microfabrication system can also apply the SR-induced photo-chemical reaction to direct etching of fluorinated polymer molecules such as polytetrafluoroethylene (PTFE) and polytetrafluoroethylene-co-perfluoroalkoxy vinyl ether [11-12]. PTFE has big potential for various applications, such as chemical, bioscience, electronics and environmental applications, for its electrical, chemical, mechanical and thermal properties. Due to its property microfabrication of PTFE with high precision has been difficult so far by the use of conventional machining, molding, and semiconductor processes. In order to accomplish wider practical applications of PTFE, microfabrication with large work-area is inevitable. We have demonstrated the PTFE microfabrication using the developed X-ray Microfabrication System and investigated the processing characteristics of PTFE direct etching.

At the first step, processing characteristics of the PTFE direct etching using SR had been studied. In the experiments, relatively high-energy region of 2 to 6 keV and 2 to over 10 keV were used at the condition of storage electron-beam energy of 1.0GeV and 1.5GeV, respectively. To investigate heating effects during X-ray exposure, large-area hotplate was mounted onto the stage and PTFE substrates, which cleaned with methanol, were attached on the hotplate to face the X-ray beam.

Figure 6 shows For the lower dose of 55 mA·hr the irradiated surface shows very smooth and fine morphology. On the contrary, there were found bubble-like structures at the higher dose of 165 mA·hr. The morphology is closely related to the etching mechanism as speculated below. As shown in Figure 7, it can be speculated that melting of PTFE less than original melting point occurs by SR irradiation, because high energy soft-x-ray photons induce continuous decomposition of PTFE. The volatile decomposed fragments of PTFE desorb from the SR-irradiated surfaces(Fig. 7(a)). As x-rays penetrate into PTFE substrate deeply, the bond-brake progresses in deeper part of the substrate. Furthermore, as elevated heat

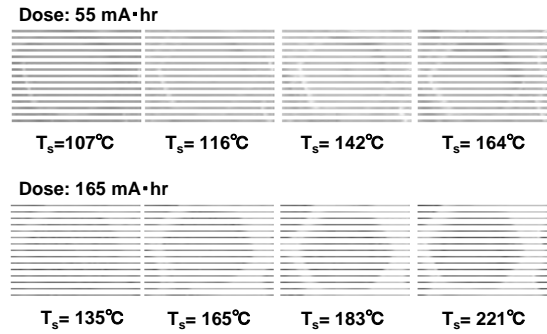


Figure 6: SEM images of each etched surface irradiated by SR with different substrate temperature and x-ray doses.

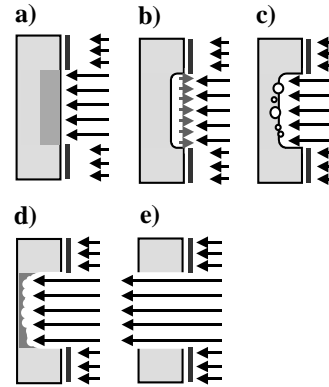


Figure 7: Speculated mechanism of PTFE etching; (a) PTFE decomposition, fragment desorption and decrease of melting point, (b) formation of melting block at the SR-irradiated area, (c) growth of the bubbles in melting block, (d) continuous etching of melting block by SR-induced reaction and thermal desorption, (e) finish of PTFE etching at SR-irradiated area.

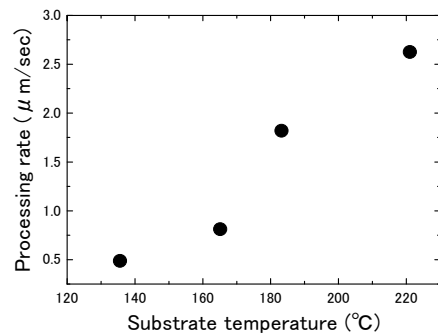


Figure 8: Etching rate dependence on substrate temperature.

contributes to rapid diffusion of decomposed PTFE molecules, it leads to the formation of large melting block expanding in entire exposed area (Fig. 7(b)). This melting of PTFE was supposed to result in the abrupt rate increase around 165 degrees as shown in Figure 8. Decomposed fragments will agglutinated and results in the growth of the bubbles in melting block (Fig. 7(c)). Etching of melting block by SR-induced reaction and thermal desorption continuously progresses during these steps and finally the irradiated part will be selectively etched (Fig. 7(d,e)). By these processes, PTFE will be precisely etched by the use of developed lithography system.

Next, the PTFE micro capillary filters with functions as microvalve, micromixer, and microreactor, were fabricated.

Figure 9 is SEM images of fabricated PTFE filter with about two thousand arrayed micro capillaries. The thicknesses and capillary diameter are ranging from 130 to 2000  $\mu\text{m}$  and 25 to 40  $\mu\text{m}$ , respectively so the maximum aspect ratio of capillary was 80. Patterning to A5 size PTFE sheet using wet-etched stencil mask was also demonstrated. It is useable for large-area microstructure applications such as lab-on-a-chip devices for medical and environmental high throughput analysis.

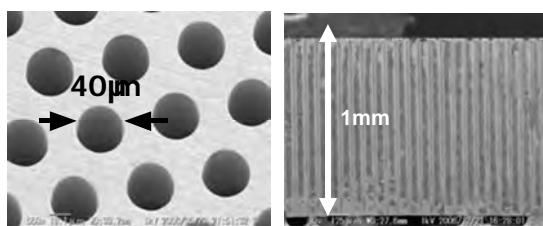


Figure 9: SEM images of fabricated PTFE filter with about two thousand arrayed micro capillaries.

### 2.3 Stacking of Microstructure using Direct Bonding and Nanoimprint Technique

The next process following after deep x-ray lithography, molding process was investigated using nanoimprint technique. Figure 10 shows the SEM images of the microchannel structure of micro capillary electrophoresis (MCE) chip for DNA analysis formed after molding of PMMA sheet by nanoimprint apparatus. The accuracy of the line dimension was less than 4% from the nickel mold inserts. And the surface roughness of the micro channel wall was less than few nm, which show the enough precision for assembly the whole DNA chip structure with multiple functions. In order to achieve the microsystem with desired functions, the assembly of the individual micro parts is inevitable. We have attained the assembly of the plastic micro parts by the

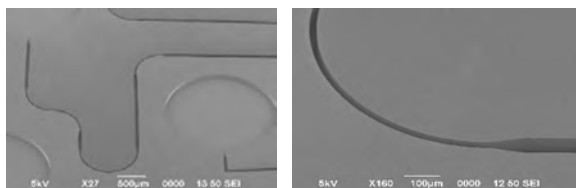


Figure 10: SEM images of the micro channel structure of MCE.

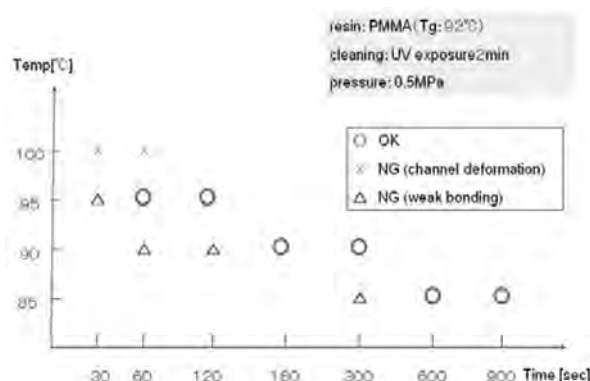


Figure 11: The result of the trials for fusion bonding.

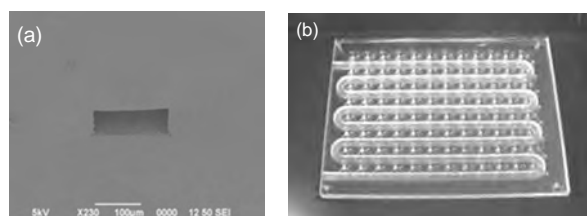


Figure 12: Outside view of the stacked structure of chip for DNA analysis.

use of the direct fusion bonding using nanoimprint apparatus to press the stacked molded structures in head loads. The fusion bonding without binding agent is necessary to avoid the inclusion of the binding agent into the micro fluid channel and to attain the dimension accuracy, which is degraded by the insertion of binding layer with low thickness stability. The fusion bonding of each three PMMA layer; top layer of a sample injection, second electrodes layer for DNA amplification and separation with 96 MCE units, and bottom heat exchanger layer, was demonstrated after some treatments of the bonding surface. Figure 11 shows the result of the trials for fusion bonding of two PMMA layers at different temperature and bonding time. The cross sectional SEM images as shown in Figure 12(a) shows the sealed microchannel with no defects and air bubble at the sealed interface and Figure 12 (b) shows the whole outside view of the stacked structure of chip with 96 MCE units for DNA analysis, which size is 88mm x 130 mm[13].

## 3 APPLICATION TO BIO MICROSISTEMS

### 3.1 Proposal of Bio Microreactor with Vertical Chemical Operation

The automation of bio-operations has become a key subject to realize point-of-care (POC) diagnostics and high throughput screenings (HTS) of various matters, such as medicine, DNA, proteins in post-genome analysis, products from immunoassays. From this point of view, "Lab on Chip" system, on which multiple chemical operations are sequentially performed through microfluidic components have been

attracted great attentions, because of their leading features such as compactness, small sample volume, fast and precisely controlled reaction, high analysis sensitivity, shortage of required time, reproducibility of output data, and low cost reliance. Such properties originated from down sizing of fluidic channels and components integrated monolithically which results in a large surface-area-to-volume ratio, a rapid thermal diffusion, a high pressure gradient, a high reagent

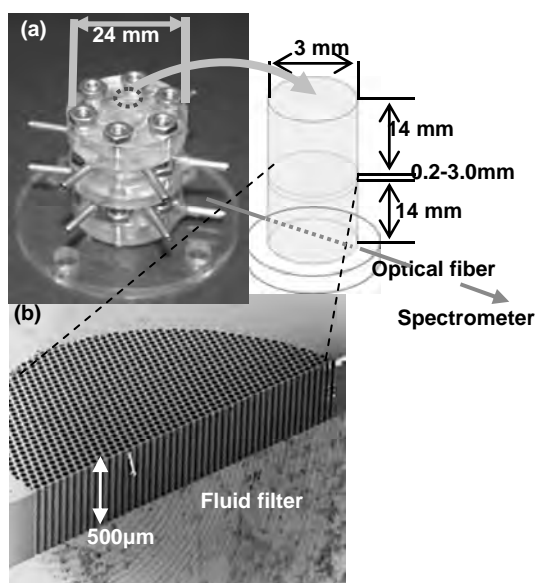


Figure 13: Out view of the vertical reactor with capillary bundle structure.

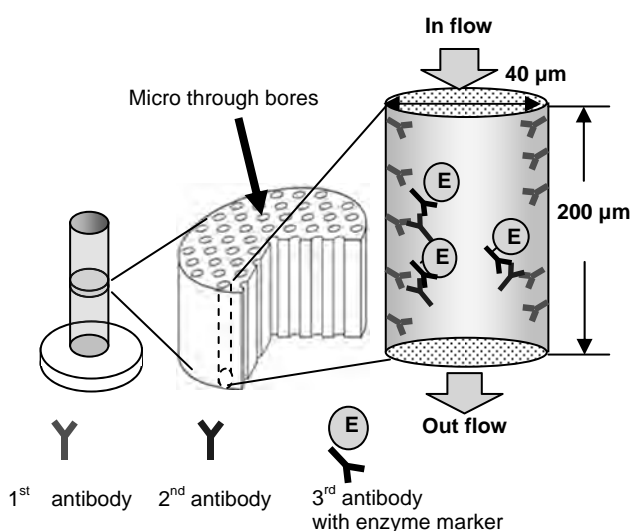


Figure 14: Scheme of the high sensitive ELISA analysis using immunoreaction arisen with the antibody stacks immobilized inside the micro capillary wall.

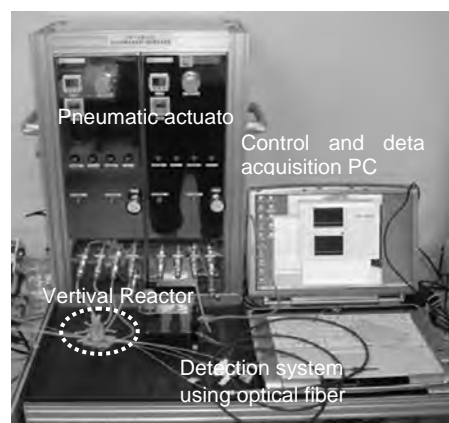


Figure 15 : Out view of the automatic ELISA system using proposed vertical immuno reactor fabricated by SR lithography.

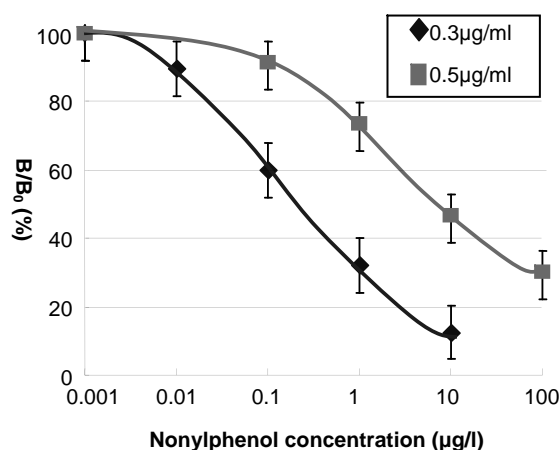


Figure 16: Calibration curve of nonylphenol concentration in the competitive ELISA.

solution concentration, and a mechanical toughness. However, typical structure of the conventional “Lab on Chip” systems assembled on a two-dimensional planar substrate has restrictions of integration of every fluidic components necessary for attaining whole sequential chemical operations specified in an analysis and synthesis.

Achieving 3D integration of multiple chemical modules and these interconnections within a finite small space will results in the integration of multiple functions which composes total sequential chemical operation, and will develop several major application fields, such as POC diagnostics, HTS of the matters, fine chemical synthesis, combinatorial synthesis.

As the first step to achieve 3D integration of microfluidics, we proposed and fabricated a new chemical reactor with a vertical fluid flow operation. As shown in Figure 13, the reactor utilizes fluid filter in which thousands of micro-through-bores

are bundled, which sustains the liquids loaded from the first upper unit reservoir. For the step of the transportation of the sustained liquids towards the lower unit reservoir, pneumatic pressure will be loaded on the surface of the liquids. In the first step of loading of the reagents from the upper unit reservoir, different reagents are not mixed sufficiently due to the low Reynolds number of the reservoir. By the use of this fluid filter, it is assumed from the reaction rate measurement and computational fluidic dynamics simulations that different reagents are mixed entirely in a few milliseconds during their transportation from upper to lower reservoir and rapid chemical reactions can also be achieved; whereas, this filter can stock the reagent solutions with antibodies immobilized on the surface of the micro-through-bores, at which immuno reaction for ELISA occurs as shown in Figure 14 (sandwich method). We investigated the possibility of the analysis using the proposed vertical micro reactor for competitive enzyme-linked immunosorbent assay (ELISA), which enable highsensitive detection of an endocrine disrupter (nonylphenol) by a series of vertical fluidic operation. In this analysis, competition between nonylphenol and nonylphenol-Horseradish-peroxidase conjugate occurs at the binding of these molecules to anti-nonylphenol monoclonal antibody (anti-NP-antibody) immobilized on surface of the micro through bores as shown in Figure 9. In the assay using filters pretreated with 0.3  $\mu\text{g/ml}$  of anti-NP-antibody, even at 0.01ng/ml of free NP, we still observed the inhibition of the binding ( $B/B_0=90\%$ ). Whole analysis protocol have been performed using automatically operating system shown in Figure 15. Under this condition, calibration curve of NP was obtained at the range of 0.01-10ng/ml as shown in Figure 16. This sensitivity was two orders higher than the sensitivity (5-100 ng/ml) obtained by ordinary ELISA using 96-wells-micro-titer plate and the same anti-NP-antibody. These assays gave reproducible results, reactor to set at the centers of the filters[14-15].

### 3.2 3D Micro Fluidic Network

The miniaturized analysis chip such as microchip electrophoresis have been well developed, however the micro

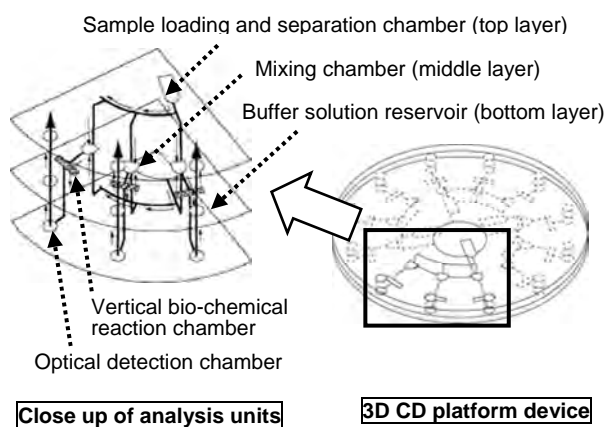


Figure 17: Schematic diagram of a new CD-like microfluidic platform with 3D fluid networks.

chemical systems with whole bio-chemical processes, including sample pre-treatment, have not been developed, while it requires much efforts and time over separation and detection. The key-technology for the solution is assembly and interconnection technologies because seamless functional connection of various devices is necessary to achieve totally automated microchip systems. The various chemical operations must be realized on one platform to realize totally automated bio-process. We adapted proposed "3D micro prototyping process" to the achievement of such advanced systems and have confirmed the advantages of 3D micro-integration of chemical functions in one chip for DNA analysis and some immunoassay applications. We proposed 3D fluidic platform system in which total chemical unit operation necessary to achieve without human operations can perform automatically, which brings high analysis sensitivity and less total analysis effort and required time. In this concept whole procedure for immunoassay can be achievable by stacking multiple CD fluids with individual functions corresponds to each sequential step for bio-chemical operation to cover whole procedure for assay. This concept is shown as the schematic diagram of a new CD-like microfluidic platform with 3D fluid networks in Figure 17. In this system only necessary manual operation is loading of sample and reagent solutions into inlets. The analysis processes typically start with this sample purification followed by some sample preparation dilution and amplification. The purified samples are then mixed with buffer solutions containing another reagents such as enzyme-labelled haptens by increasing the rotation speed of CD. The reagents are pre-loaded in the other chamber formed on the bottom disk of the stack structure. The specific volumes of reagent solutions and sample liquids are automatically injected into mixing chamber located in the middle disk of the stacked structure consists of three-dimensionally crossing channel network, and dispensed to desired volume ratios for designed protocol. For complete mixing of sample and reagents the high-efficiency mixing device is necessary. For this purpose a 3D mixer with opposed-capillary structure is feasible at the mixing chamber. The mixture will next injected into biochemical reaction chamber with antibody immobilized 3D microstructure. Specific area of immobilized antibody become to be several decades times larger than conventional planar reactor microchannels, which results in the enhancement of the reaction rate and the analysis sensitivity, reproducibility of the immuno systems. The solution of product of bio-chemical reaction will then injected into detection chamber located after the reaction chamber and amount of the product will measured by using optical detection. Normally, optical path of micro channel on a conventional planer fluidic platform, which corresponds to the depth of the fluidic channel, is less than 100 micron and it has restrictions for detection such as difficulty of alignment and small signal due to the lack of optical path for absorption and fluorescence detection. On the other hand stacked CD structure can increase optical path up to several millimetres by forming detection channel across the stacked CDs.

### 3.3 Application of 3D Fluidic System to High Sensitive Elisa Immunoassay

The other benefits of the automation are realization of highly precise and reliable operations by reducing human errors or

mistakes. One promising way to realize automation for immuassay is to utilize CD-like microfluidic platforms as mentioned above. In this section we will describe the detailed structure and protocol for ELISA with high-sensitive and high-speed, and high-reliable property of 3D CD platform devices. For automatic ELISA, the liquids, sample, wash, substrate, and reaction aborting solution are pre-loaded into reservoirs and sequentially injected into 3D bio-reaction chamber by spinning CD. For the first sequencing, the mixture of sample and enzyme conjugated hapten will be injected and competitively conjugate with 1<sup>st</sup> antibody immobilized on the

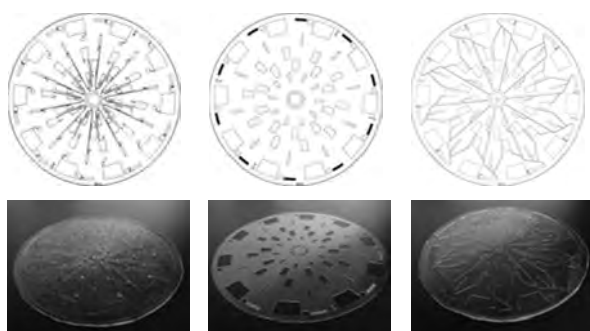


Figure:18 Illustration and photographs of designed and fabricated CD platform consist of three layers

surface of 3D microstructure. After incubation, the washing buffer will injected from second reservoirs by accelerating hundreds rpm, and excess samples will be washed away. The next, substrate reagent to quantify the extent of competitive reaction of sample and enzyme labelled haptens will be injected from third reservoir into reaction chamber and incubated to amplify the signal of products according to designed protocol. Finally the enzyme reaction will stopped by injecting reaction stopping solution released from fourth reservoir, and amount of products will measured in optical chamber and calibration curve will obtained. Figure 18 shows illustration and photographs of designed and fabricated devices. The devices consist of three-stacked layers with ten assay units for parallel assay of 10 samples. Each unit consists of four liquid loading reservoirs and biochemical chamber with filter structure as mentioned at chapter 3.1 and optical detection chamber. All CDs are aligned and stacked together by using self-adhesion of poly-dimethylsiloxane (PDMS). The thickness of the reservoirs and chambers set to adjust the suitable sample, reagent volumes and optical path length of the reaction products for UV absorption and fluorescence. The high aspect ratio structure of liquid loading reservoir is effective to integrate assay units by reducing planar area of reservoirs. To demonstrate the automatic sequencing in 3D CD platform, we loaded protein solution into the reservoirs (0.1% bovine serum albumin phosphate buffer solution: 0.1%BSA) and CD platform is spun for the sequencing. The snapshot images are obtained by strobe scope system to observe and measure the burst frequency of each chamber. The schematic illustration of strobe scope system is shown in Figure 19. The optical sensor will generate

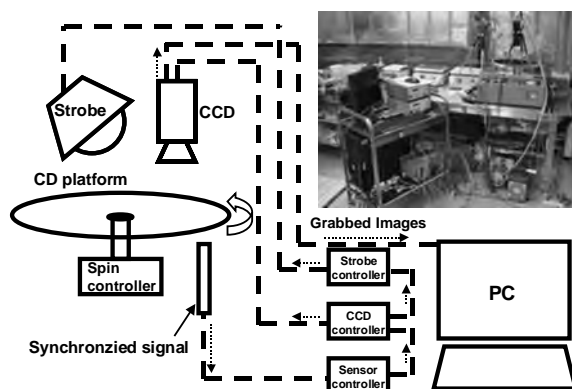


Figure :19 Schematic illustration and photograph of strobe scope system

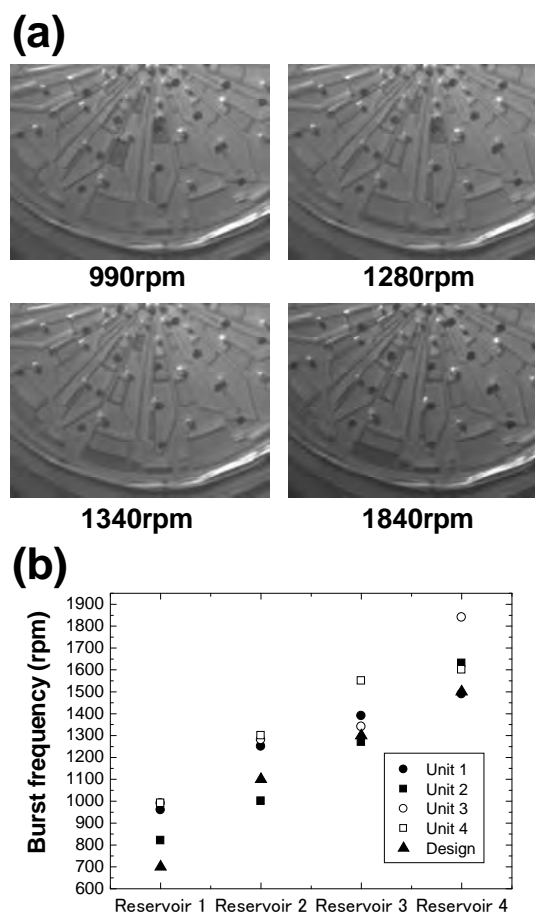


Figure: 20 (a) Images of flow sequencing of BSA solution and (b) measured burst frequency

the trigger signals for the synchronized control of CCD and strobe. The taken images are automatically grabbed with time information into PC and burst frequency was calculated by checking holding state and the time. Figure 15 (a) show the obtained images of automatic flow sequencing in 3D CD platform and measured burst frequencies are shown in Figure 20 (b). As shown in Figure 20 (b) we succeeded in sequential transportation of BSA solution in four individual reactor units in 3D CD-like platforms. The result suggests the proposed 3D microfluidics platform is available to automated ELISA analysis.

#### 4 SUMMARY

3D micro prototyping process have been developed using synchrotron radiation (SR) lithography and nano-imprinting technique. Large-area patterning up to A4-size area was also successfully performed with a highly uniform pattern thickness. The X-ray microfabrication system can also apply the SR-induced photo-chemical reaction to direct etching of fluorinated polymer molecules. The stacking process as the device assembly and interconnections for obtained micro structures is also demonstrated using some types of surface treatment and succeeding nano-imprinting techniques for assembling 3D functional fluidic structure. We adapted proposed "3D micro prototyping process" to the achievement of 3D micro fluidic platforms and have confirmed the novel properties of high analysis sensitivity, speed, and low reagent consumption. for some assay applications. An enzyme linked immunosorbent assay method has been investigated using proposed micro 3D fluidic platforms in which thousands of micro capillary are integrated as a fluid control filter and bio-chemical reaction space in 3D fluid networks. Drastic improvement of the analysis sensitivity and decreasing the total analysis effort and required time have found in the applications for the environmental analysis. We also succeeded in sequential transportation of BSA solution in four individual reactor units in 3D CD-like platforms.

#### 5 ACKNOWLEDGMENTS

This work has performed with the aides of New Energy Development Organization, Japan Society for the Promotion of Science, and COE program of Hyogo Prefecture, Japan.

#### 6 REFERENCES

- [1] A. Ando, T. Hattori, K. Hosono, K. Kanda, H. Kinoshita, S. Matsui, H. Mekaru, M. Niibe, Y. Utsumi and T. Watanabe : Journal of The Japanese Society for Synchrotron Radiation Research, **15**, (2002) p. 336.
- [2] Y. Utsumi, and T. Kishimoto, Journal of. Vacuum. Science and Technologies. B, **23**, 6, 2903-2909 (2005).
- [3] D. Fukuoka, and Y. Utsumi, p387., International Conference on Electronics Packaging 2008, JAPAN, June 2008
- [4] Y. Utsumi, T. Ikeda, M. Minamitani, .K Suwa, p.125., 7th International Workshop on High-Aspect-Ratio Micro-Structure Technology 2007, FRANCE, June 2007
- [5] F. J. Pantenburg, S. Achenbach and S. Mohr, Microsystems Tech. **4**, (1998) 89.
- [6] E. W. Becker, W. Ehrfeld, P. Hagmann, A. Maner and D. Munchmeyer, Microelectronic Eng. **4**, (1986) 35.
- [7] W. Ehrfeld : Proc. High Aspect Ratio Micro Structure Technology, 2001,(2001) p. 05.

- [8] J. Goettert, G. Aigeldinger, Y. Desta, Z.L.Ling, and L. Rupp, Proc. Synchrotron Radiation Instrumentation, 2001, (2001) p. 102.
- [9] Y. Utsumi, M. Minamitani and T. Hattori : Electrical Engineering in japan , **165**, **1** (2008) p.52.
- [10] K. Fujiwara, Y. Ukita, M. Takeo, S. Negoro, T. Kanie, M. Katayama, and Y. Utsumi, p.297., 7th International Workshop on High-Aspect-Ratio Micro-Structure Technology 2007, FRANCE, June 2007
- [11] Y. Ukita, M. Kishihara, Y. Haruyama, K. Kanda, S. Matsui, K. Michiji, and Y. Utsumi, Japanese Journal of Applied Physics, **47**, pp. 337-341 (2008).
- [12] M. Kishihara, Y. Ukita, Y. Utsumi, and I. Ohta, p.301., 7th International Workshop on High-Aspect-Ratio Micro-Structure Technology 2007, FRANCE, June 2007
- [13] Y. Utsumi, M. Minamitani and T. Hattori : Electrical Engineering in japan , **165**, **1** (2008) p.52.
- [14] Y. Utsumi, Y. Ukita, and T. sano, 51st International Conference on Electron Ion and Photon Beam Technology and Nanofabrication, USA, May 2007
- [15] K. Matsui, I. Kawaji, Y. Utsumi, Y. Ukita, T. Asano, M. Takeo, D. Kato, and S. Negoro, Journal of Bioscience and Bioengineering, **104**, **4**, 347-350 (2007).
- [16] M. J. Madou and G. J. Kellogg, Proc. SPIE, **3259**, 1998, p80-93
- [17] S. Lai, S. Wang, J. Luo, L.J. Lee, S-T. Yang, and M. J. Madou, Anal. Chem., **76**, 1832-1837, 2004
- [18] Y-K. Cho, J-G. Lee, J-M Park, B-S. Lee, Y. Lee, and C. Ko, Lab. Chip, **7**, 565-573, 2007.



Service Robotics and Mechatronics

Selected Papers of the International Conference on  
Machine Automation ICMA2008

Shirase, K.; Aoyagi, S. (Eds.)

2010, XII, 392 p., Hardcover

ISBN: 978-1-84882-693-9